A photosynthetic rotating annular bioreactor (Taylor–Couette type flow) for phototrophic biofilm cultures

A. Paule [a,b], B. Lauga [c], L. Ten-Hage [a,b], J. Morchain [d,e,f], R. Duran [c], E. Paul [d,e,f], J.L. Rols [a,b,*]

[a] Université de Toulouse, UPS, INP, EcoLab (Laboratoire d'écologie fonctionnelle et environnement), 118 route de Narbonne, F-31062 Toulouse, France
[b] CNRS, EcoLab, F-31062 Toulouse, France
[c] Equipe Environnement et Microbiologie, Institut Pluridisciplinaire de Recherche sur l'Environnement et les Matériaux - IPREM, UMR 5254 CNRS/UPPA, IBEAS, Université de Pau et des Pays de l'Adour, BP1155, F-64013 Pau, France
[d] Université de Toulouse, INSA, LISBP, 135 Avenue de Rangueil, F-31077 Toulouse, France
[e] INRA, UMR792, Ingénierie des Systèmes Biologiques et des Procédés, F-31400 Toulouse, France
[f] CNRS, UMR5504, F-31400 Toulouse, France

Keywords:
Rotating annular bioreactor
Taylor–Couette type flow
T-RFLP
Phototrophic biofilm
Microbial community
Photobioreactor

In their natural environment, the structure and functioning of microbial communities from river phototrophic biofilms are driven by biotic and abiotic factors. An understanding of the mechanisms that mediate the community structure, its dynamics and the biological succession processes during phototrophic biofilm development can be gained using laboratory-scale systems operating with controlled parameters. For this purpose, we present the design and description of a new prototype of a rotating annular bioreactor (RAB) (Taylor–Couette type flow, liquid working volume of 5.04 L) specifically adapted for the cultivation and investigation of phototrophic biofilms. The innovation lies in the presence of a modular source of light inside of the system, with the biofilm colonization and development taking place on the stationary outer cylinder (onto 32 removable polyethylene plates). The biofilm cultures were investigated under controlled turbulent flowing conditions and nutrients were provided using a synthetic medium (tap water supplemented with nitrate, phosphate and silica) to favour the biofilm growth. The hydrodynamic features of the water flow were characterized using a tracer method, showing behaviour corresponding to a completely mixed reactor. Shear stress forces on the surface of plates were also quantified by computer simulations and correlated with the rotational speed of the inner cylinder. Two phototrophic biofilm development experiments were performed for periods of 6.7 and 7 weeks with different inoculation procedures and illumination intensities. For both experiments, biofilm biomasses exhibited linear growth kinetics and produced 4.2 and 2.4 mg cm^{-2} of ash-free dry matter. Algal and bacterial community structures were assessed by microscopy and T-RFLP, respectively, and the two experiments were different but revealed similar temporal dynamics. Our study confirmed the performance and multipurpose nature of such an innovative photosynthetic bioreactor for phototrophic biofilm investigations.

* *Corresponding author*. Université de Toulouse, UPS, EcoLab (Laboratoire d'écologie fonctionnelle et environnement), 118 route de Narbonne, F-31062 Toulouse, France. Tel.: +33 0 6 24 38 19 04; fax: +33 0 5 61 55 60 96.
E-mail address: rols@cict.fr (J.L. Rols).

doi:10.1016/j.watres.2011.09.007

1. Introduction

Environmental phototrophic biofilms are microbial aggregates occurring on solid substrates and consisting of heterotrophic micro- and meio-organisms and phototrophic micro-organisms embedded in an extracellular polymeric substance matrix. The structure and functioning of microbial communities from phototrophic biofilms are mediated by abiotic factors such as nutrient availability (Hillebrand and Sommer, 2000a), light (Boston and Hill, 1991), substrate types (Murdock and Dodds, 2007), hydrodynamics (Battin et al., 2003), and by biotic interactions such as competition (Jackson et al., 2001) or predation (Bourassa and Cattaneo, 1998). Biofilm development has been demonstrated to be associated with population succession processes over biofilm maturation, both for the algal (McCormick and Stevenson, 1991) and the bacterial (Jackson et al., 2001; Lyautey et al., 2005) compartments.

To understand how the abiotic and biotic factors (alone or combined) influence the microbial community structure, its dynamics and the biological succession processes during phototrophic biofilm development, the best approach is to use laboratory-scale systems simulating environmental conditions under different levels of experimental control.

Various large and small-scale laboratory systems designed to investigate phototrophic biofilms are described in the literature (e.g. Battin et al., 2003; Singer et al., 2006). Among them, rotating annular bioreactor (RAB) designs have been suggested as a powerful tool to study the effects of environmental change on biofilm development (Neu and Lawrence, 1997). It has been shown that the hydrodynamic conditions at local level influence the composition and the structure of biofilms (Besemer et al., 2007). The geometry of RABs allows to provide a constant shear stress distribution and cultivation of biofilm under turbulent flow environments (Characklis, 1990). While RABs are described as completely mixed reactors for the liquid phase, a previous study showed heterogeneity in the growth of biofilm related to reactor geometry (Gjaltema et al., 1994). In the last decade, Lawrence et al. (2000) have developed a RAB (liquid working volume of 0.5 L) for the cultivation of phototrophic biofilms, used to investigate the various effects of environmental change occurring in a river (Chénier et al., 2003; Lawrence et al., 2004). The main shortcomings of this RAB are its small size which limits the number of possible analyses and replicates, the external illumination, and the biofilm growing on the rotating inner cylinder.

The objectives of our study were (i) to design and describe a new prototype of RAB (Taylor–Couette type flow) specifically intended for the cultivation and investigation of phototrophic biofilms adapted from an RAB design for biological waste water treatment (Coufort et al., 2005), (ii) to assess the applicability of this prototype in phototrophic biofilm production and (iii) to analyze the phototrophic biofilm dynamics. Innovations of our modified RAB were the presence of a modular source of light inside the system and the biofilm colonization on the stationary outer cylinder. Two cultivation experiments were performed for periods of 6.7 and 7 weeks with different inoculation procedures and illumination intensities.

2. Material and methods

2.1. Experimental setup

Phototrophic biofilm culture experiments were conducted in a new prototype of a photosynthetic rotating annular bioreactor (RAB) with Taylor–Couette type flow (Arias, Toulouse, France).

2.1.1. RAB characteristics

The RAB consisted of two concentric cylinders, a stationary outer cylinder made of polyvinyl chloride and a rotating inner cylinder made of poly(methyl methacrylate) (PMMA) (Fig. 1A and B). A schematic diagram and the geometric characteristics of the RAB are given in Fig. 1C and D, respectively. This prototype presents the specificity of having (i) a modular source of light inside the system, protected by an internal water-tight cylinder made of PMMA and adjusted by changing the quality and number of the fluorescent tubes (1–8) and the frequency of light/dark cycles, and (ii) a flow generated in the annular gap (width 18.5 mm) through the rotation of the inner cylinder modulated by different motor speeds. The inside of the external cylinder supports 2 rows of 16 removable polyethylene plates or sampling units ($l \times h = 50 \times 100$ mm; 5 mm wide) for biofilm sampling. The total surface available for the biofilm colonization of plates in the RAB is 0.16 m^2. To limit the occurrence of edge effects on the development of biofilm, the rows of plates were positioned at half height in the bioreactor. The plates were curved to avoid perturbation of the flow. To prevent biofilm growth on the back, upper part and leading edge of the plates, these surfaces were covered by adhesive bands during the experiments which were removed before the biofilm analyses. All bioreactor components were cleaned, with diluted detergent (Decon, 10%) for the plates, the outer cylinder and the port, or with hydrogen peroxide (30%) for the inner cylinders, and then rinsed with demineralized water. To prevent unwanted biofilm formation that could attenuate the light intensity and modify its spectrum, the surfaces of the rotating inner and internal water-tight cylinders were cleaned manually once a week. This step of 15 min required to collect the liquid contained in the RAB before opening, and allowed, if necessary, to collect some plates for biofilm analyses. Once finished, the bioreactor was closed and refilled with the collected liquid.

2.1.2. RAB hydrodynamic behaviour

The RAB was operated at 80 rpm, which corresponds to a Reynolds number $Re = r_i.\Omega.(r_e - r_i)/\upsilon = 17{,}040$ and Taylor number $Ta = Re.[(r_e - r_i)/r_i]^{1/2} = 6970$ where r_i is the inner cylinder radius (m), r_e is the outer cylinder radius (m), Ω is the angular speed (rad s^{-1}) of the inner cylinder, and υ is the cinematic viscosity of the fluid (m^2 s^{-1}) (tap water). According to the literature, this value of Taylor number indicates a turbulent vortex flow with stacked axisymmetric toroidal vortices (Desmet et al., 1996). Bioreactor with Taylor–Couette type flow exhibits different flow regimes (e.g. Couette, vortex flow, turbulent vortex flow, turbulent flow…) depending on the rotational speed of the inner cylinder. In the RAB designed

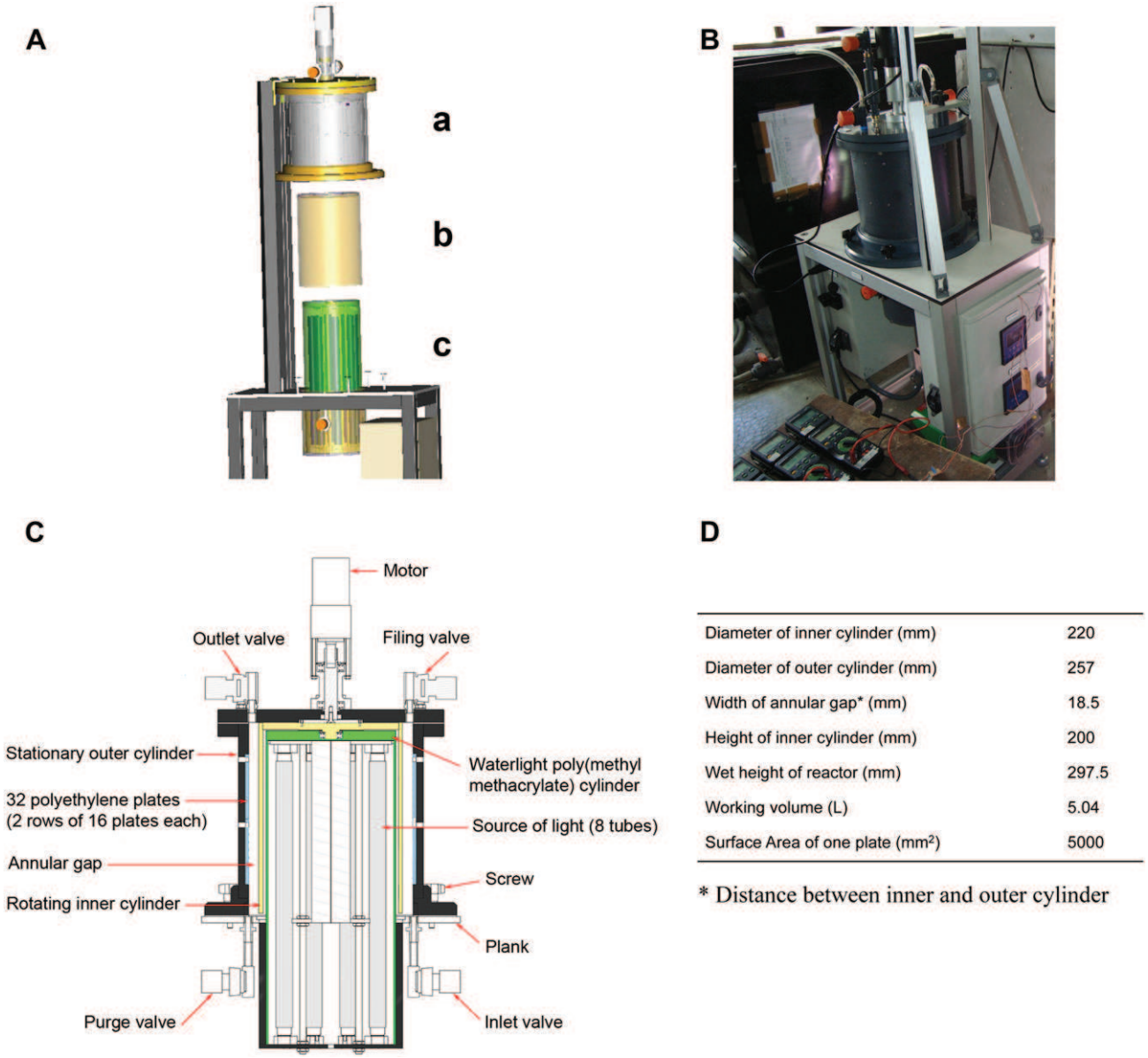

Fig. 1 – Setup of the photosynthetic rotating annular reactor (RAB) with Taylor–Couette type flow. (A) 3D representation of different parts composing the RAB, a : the stationary outer cylinder, b : the rotating inner cylinder and c : the light source protected by an internal water-tight cylinder, (B) photograph of RAB, (C) schematic diagram of RAB and (D) geometric characteristics of RAB.

for the present work, the objective was to work with turbulent vortex flow with spatial periodicity and rotational speed of the inner cylinder high enough to avoid the settling of micro-organisms in the annular gap. In this context, the rotational speed of the inner cylinder was set to at least 80 rpm. The RAB hydrodynamic was studied experimentally at the reactor scale by the tracer method and local flow properties were obtained through computational fluid dynamics (CFD) simulation.

2.1.2.1. *Residence time distribution.* The general mixing behaviour in the RAB was investigated experimentally using the pulse tracer method (10 mL of NaCl solution at 0.16 g mL^{-1}) to determine the residence time distribution (RTD). The experiment was conducted for two different rotational speeds, 80 and 170 rpm, and the inlet throughput (tap water at 20 °C) was supplied at $Q = 26$ mL min^{-1} for a working volume in the RAB of $V = 5.04$ L. The conductivity of the fluid was recorded at the outlet for 15 h (corresponding to 5 times the average residence time) with a specific probe (conductivity meter 524, CRISON, SELI, probe response time of 2 s) located in an agitated cell (30 mL) positioned at the outlet valve, in absence of biofilm and without illumination in the RAB.

RTD curves, defined as dimensionless concentration ($E(\theta)$) versus dimensionless time (θ), were obtained from the outlet conductivity concentration data:

$$E(\theta) = c(t)/c(0) \quad (1)$$

where θ is given by the ratio t/τ with $\tau = V/Q$, c(t) and c(0) are respectively the tracer concentrations at time t and time 0 for which c(0) results from an instantaneous mixing of the injected tracer. The experimental RTD curves were compared with the RTD curve obtained from a mathematical model of reactor as described by Sugiharto et al. (2009).

2.1.2.2. Computational study of hydrodynamics. Numerical simulation was performed to evaluate the flow pattern within the annular space and the characteristic turbulent scales. The mean wall shear stress on the external cylinder and the axial average velocity profiles in the annular gap were extracted from the simulations. The computational study was performed using the CFD software Fluent (6.2) at the rotational speeds of 80 and 170 rpm. The first step was to draw the grid and mesh the two-dimensional domain using the Fluent preprocessor Gambit®. The simulations were run as described by Coufort et al. (2005), i.e. Reynolds Averaged Navier–Stokes equations combined with the k-ε Reynolds Stress Model, 2D-axisymmetric model in the steady state.

2.2. Experimental design

Initially, the bioreactor was run in batch culture mode for a seeding period to allow the micro-organisms to become attached before the continuous culture mode started.

2.2.1. Seeding procedures

The two biofilm cultures were achieved using two different seeding procedures. Seeding was conducted for 48 h, once for culture 1 and twice for culture 2. For culture 2, the two seeding phases were separated by a 24-hour period where the RAB operated in continuous culture mode. During the seeding phases, the bioreactor ran in closed recirculation, connected to an aquarium (10 L) where the inoculum was incubated. The aquarium was illuminated by fluorescent lamps including one cool daylight (F18W/GRO, Sylvania, Germany) and one fluora (F18W/54, Gt Britain) tubes, supplying average illumination values of 32 ± 3 μmol s^{-1} m^{-2} with light/dark periods of 16 h/8 h. The inoculum was obtained by removing epilithic biofilms by scraping with a toothbrush, previously treated with NaOH 1N, from (i) glass slides as previously described (Paule et al., 2009) placed in the experimental channel of our laboratory for culture 1 or (ii) various river stones for culture 2. Biofilm suspensions were homogenized (tissue homogenizer at 13,500 rpm, Ultra Turrax, T25) and filtered through a 250 μm and then 100 μm pore size filter (VWR) to reduce the part of the macro fauna and coarse sediments from the natural biofilms. The end of seeding phase was defined as the start of the experiment (day 0).

2.2.2. Experimental conditions

The experiment design used a thermostated reservoir (150 L, model CV 150, Japy) at 4 °C, equipped with a peristaltic pump (520S/R2 220 T/MN pump with silicon tubes ID × OD = 1.6 × 2.4 mm) which fed the RAB continuously with a synthetic culture medium. The inlet throughput was 26 mL min^{-1}, which corresponded to a hydraulic residence time in the RAB of 3.23 h. The synthetic culture medium consisted of tap water supplemented with nutrients (SiO_2, PO_4^{3-} and NO_3^-) to favour the growth of biofilm and avoid nutrient limitation. Nutrient concentrations were measured as described by Paule et al. (2009). The physical-chemical parameters (temperature, pH and dissolved oxygen concentration) were recorder using probes located in the agitated cell (30 mL) positioned at the outlet valve of the reactor. Temperature and pH were measured with a pH meter 296 WTW (electrodes sentix H 8481 HD, SCHOTT). Dissolved oxygen concentrations were measured with an oxy 296 oxymeter WTW (trioxmatic 701 sensor, WTW). Dissolved organic carbon (DOC) concentrations were measured on acidified water samples (4 μL of HCl 6N) and analyzed using a carbon analyser at 680 °C (Shimadzu, Model TOC 5000H). Table 1 summarizes the chemistry of the feed waters for both cultures. For culture 2, the pH of the culture medium was adjusted to 7.0 using sulphuric acid (95%).

The inside of the RAB was illuminated by fluorescent lamps including cool daylight (Osram L15W/865 Luminux, Germany) and fluora (Osram L15W/77, Germany) tubes in equal proportions, with light/dark periods of 16 h/8 h. Fluora tubes emit in the visible red, which enhances photosynthesis. At the center of the cylinder containing neon tubes, a cylinder of PMMA is positioned to improve the distribution of the light. Two neon tubes were used for culture 1 and 4 for culture 2. The illumination was measured as air photosynthetically active radiation (PAR) irradiance level by using a flat quantum sensor (model LI-189, LI-COR, Inc - Lincoln - Nebraska) and average recorded values were 130 ± 20 and 180 ± 10 μmol s^{-1} m^{-2} for cultures 1 and 2 respectively. The PAR irradiance level was measured in the air because of the small size of the annular gap, and at a distance from the rotating inner cylinder equivalent to the annular gap. The values of illumination were chosen in this study in response to two constraints. The number of neon tubes (2 and 4) is a good compromise to maintain illumination homogeneity (the fewer lamps are used, the less uniform the light field is) and to prevent an increase of temperature generated by the presence of neon tubes (the RAB is not thermostated).

2.2.3. Biofilm characterization

The development of biofilm was monitored for 6.7 (culture 1) and 7 (culture 2) weeks. Biofilm cultures were carried out between June 11 and July 30, 2008 for culture 1 and between

Table 1 – Physical-chemical characteristics of the synthetic water used to feed the rotating annular bioreactor during cultures 1 (C1) and 2 (C2). DOC = dissolved organic carbon concentration.

	PO_4^{3-}–P (mg L^{-1})	NO_3^-–N (mg L^{-1})	SiO_2 (mg L^{-1})	Conductivity (μS cm^{-1})	DOC (mg L^{-1})	pH
C1	0.357 ± 0.03	6.3 ± 0.1	13.1 ± 0.7	311 ± 29	0.6 ± 0.2	8.0 ± 0.5
C2	0.356 ± 0.02	4.2 ± 0.2	10.9 ± 2.9	368 ± 5	1.1 ± 0.3	7.1 ± 0.2

July 23 and September 16, 2009 for culture 2. At each sampling date, 3 plates were randomly sampled to follow the biofilm development. Access to the plates required opening the bioreactor and removing working fluid. Biofilms were removed from plates by scraping with a microscope slide previously treated with alcohol. Each plate represented one replicate. Biofilms were suspended in 50 mL (culture 1) or 90 mL (culture 2) of tap water previously filtered through a 0.2 μm pore size filter (cellulose acetate membrane, Whatman) and homogenized (tissue homogenizer at 13,500 rpm, Ultra Turrax, T25). Biofilm suspension was aliquoted for the analyses of biomass descriptors, algal diversity and bacterial community structure by T-RFLP. Sampled plates were substituted by clean plates in the RAB and the newly placed plates were excluded from the following samplings.

2.2.3.1. *Biomass descriptors*. From an aliquot of initial biofilm suspension, the dry mass (DM) (aliquot of 30 mL), the ash-free dry mass (AFDM) and the chlorophyll *a* (aliquot of 10 mL) were measured as described by Paule et al. (2009).

2.2.3.2. *Algal diversity*. Algal diversity was estimated from a pool of 3 aliquots of 5 mL of homogenized biofilm suspension that was preserved in formalin solution (3%) and kept in darkness at 4 °C until counting and identification. The total density and abundance percentages were determined with an inverted microscope (Axiovert 10, Zeiss, West Germany) (Utermöhl, 1958).

2.2.3.3. *Microbial community structure*. After centrifugation (12,000 g at 4 °C for 20 min, Heraeus Multifuge) of an aliquot of 20–50 mg dry mass of the initial biofilm suspension (Lyautey et al., 2005), the pellet was stored at −80 °C until further analysis. Genomic DNA extraction was performed on the pellet using a DNeasy Plant Mini Kit according to the manufacturer's protocol (Qiagen Laboratories). The integrity of the extracted DNA was checked as described by Paule et al. (2009).

The 16S rRNA genes were amplified by PCR and the bacterial community structure was studied by T-RFLP as described by Bruneel et al. (2006) with slight modifications. The fluorescent labelled primers FAM 8F (5′-6-carboxy-fluorescein-phosphoramidite-AGA GTT TGA TCC TGG CTC AG-3′) (Eurogentec, 295 Liege, Belgium) (Lane, 1991) and HEX 1489R (5′-hexa-chloro-fluorescein-phosphoramidite- TAC CTT GTT ACG ACT TCA-3′) (Invitrogen, Carlsbad, USA) (Weisburg et al., 1991), described as universal within the bacterial domain, were used. The reaction mixture for PCR was made in a 50 μL volume containing 30 ng of template DNA, 25 μL AmpliTaq Gold 360 Master Mix (Applied Biosystems) and 0.5 μL of each primer. Amplification was carried out using an Applied Biosystems thermocycler with the following sequence: a 5 min hot start at 95 °C, followed by 35 cycles consisting of denaturation (45 s at 95 °C), annealing (45 s at 55 °C) and extension (1 min at 72 °C), and a final extension at 72 °C for 10 min. Restriction digestion was performed with HinfI.

2.3. Data analysis

T-RFLP profiles from the two cultures were compared by a web-based tool, T-Align (http://inismor.ucd.ie/~talign/) as previously described by Smith et al. (2005) with the confidence interval of 0.5. Peaks, defined as Terminal Restriction Fragments (T-RFs), were scored as present or absent from T-RFLP profiles. The difference in physical-chemical characteristics and the difference in AFDM, chlorophyll *a* and the number of T-RFs between biofilm samples were assessed with the Mann Whitney test using SPSS software 13.0. Differences were considered statistically significant at $p \leq 0.05$.

To assess changes over time in the bacterial community structure from each culture, a Principal Component Analysis (PCA) was performed from the T-RF binary data for each biofilm culture using Primer v6 software (PrimerE, Ltd, Lutton, United Kingdom). Peaks < 0.5% of the total area were excluded from the analysis and T-RFs that differed in size by 0.5 bp or less were considered to be identical. This baseline of 0.5% was defined in accordance with the approaches of Osborne et al. (2006).

Statistical analyses of PCA were run using an analysis of similarity (ANOSIM) via Past software 2.06 (Hammer et al., 2001) on Bray Curtis similarity matrices generated from binary data. This analysis generates a global *R* value in the range from 0 (completely random pattern) to 1 (completely separated groups) (Clarke, 1993). The global *R* value was considered statistically significant at $p < 0.05$ uncorrected.

3. Results

3.1. Biofilm culture conditions

Throughout the experiments and associated with daily variations and photosynthetic processes, the temperature, pH and dissolved oxygen concentration values ranged from 19 to 30 °C, from 7.5 to 10, and from 4 to 18 mg L^{-1}, respectively.

According to residual nutrient concentration values measured at the outlet of the RAB (data not shown), nutrients added in the synthetic culture medium were sufficient to support biofilm growth.

3.2. RAB hydrodynamic behaviour

This section describes the characterization of the hydrodynamic behaviour of the flow in the annular space between the inner and outer cylinders through both experimental and numerical studies, performed at two rotational speeds: 80 and 170 rpm. Similar results were observed for both rotational speeds and only the data corresponding to 80 rpm are presented here.

3.2.1. RTD experiment

Fig. 2 compares the RTD curves obtained with experimental data and predicted model simulation for one completely mixed reactor. The experimental and predicted model curves are similar. The experimental mean residence times were 209.9 and 220.8 min for rotational speeds of 80 and 170 rpm respectively.

3.2.2. Computational study of hydrodynamics

For the rotational speed of 80 rpm, Fig. 3 shows a contour plot of local velocity in the annular space computed at the scale of

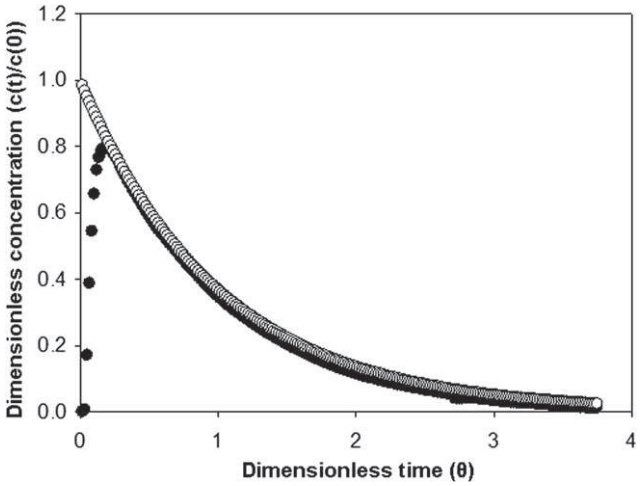

Fig. 2 – Comparison between experimental (black dots) and predicted (white dots) Residence Time Distribution (RTD) curves at 80 rpm rotational speed and 26 mL min^{-1} inlet flow. Predicted curve corresponds to model with a completely mixed reactor.

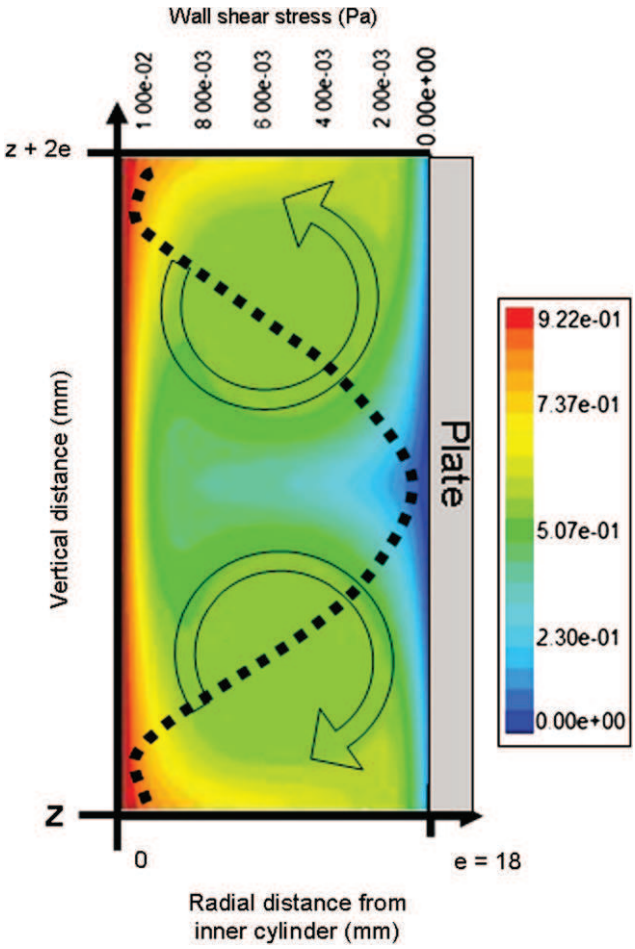

Fig. 3 – Contour plot of velocity magnitude field (m s^{-1}) in the annular space between inner (left) and outer (right) cylinders computed by CFD at rotational speed of 80 rpm, and the corresponding wall shear stress along plates placed inside the outer cylinder (e is the width of the annular gap).

two vortices, together with the outer cylinder wall shear stress for the same conditions (the dotted curve in Fig. 3). The presence of vortices produced a gradient of velocity at local scale on the walls of the cylinders. Consequently, the wall shear stress, which is directly related to the velocity gradient, was clearly non-uniform along the plate. In the zone of convergence of two vortices near the plate, the shear stress was maximal and a radial flow formed from plate to inner cylinder. The two vortices separated near the plate and the shear stress was minimal when the radial flow reached the plate.

The diameter of an individual vortex is approximately equal to the annular gap and thus the number of stacked vortices was 5.4 across the height of one plate. The magnitude of the wall shear stress along plates increased with the rotational speed of the inner cylinder ($r^2 = 0.99$). The mean values of shear stress were calculated as described by Coufort et al. (2005) and were found to be 1.11 and 4 Pa at rotational speeds of 80 and 170 rpm respectively.

Fig. 4 presents the average tangential velocity profile at a rotational speed of 80 rpm. The profile shows a decrease in tangential velocity across the inner and outer cylinders, which is characteristic of a turbulent vortex flow (Coufort et al., 2005). As a result, tangential velocity is about 0.3 m s^{-1} at the plate wall when rotational speed is 80 rpm and 0.7 m s^{-1} for 170 rpm (data not shown).

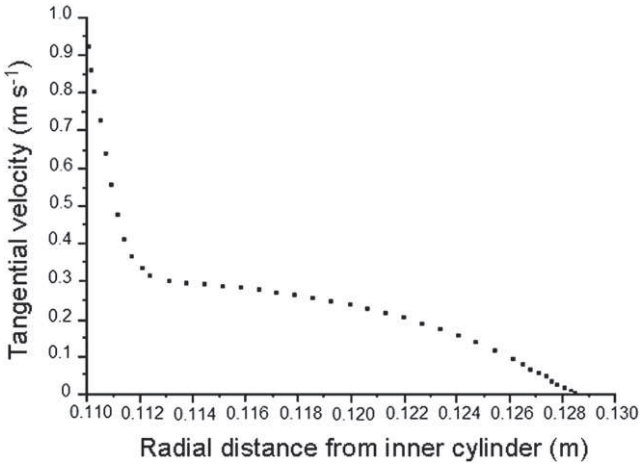

Fig. 4 – Profile of tangential velocity along a line of constant height in the annular space between the inner (left) and outer (right) cylinders computed by CFD for a rotational speed of 80 rpm.

3.3. *Biofilm analyses*

3.3.1. *Biomass descriptors*

Fig. 5 illustrates the biofilm colonization of plates over both experiments. The first colonization states occurred on the ridges of plates. Biofilm biomass as expressed by AFDM and chlorophyll *a* presented similar linear growth patterns, giving a biomass peak of 4.2 and 2.4 mg AFDM cm^{-2} and 0.05 and

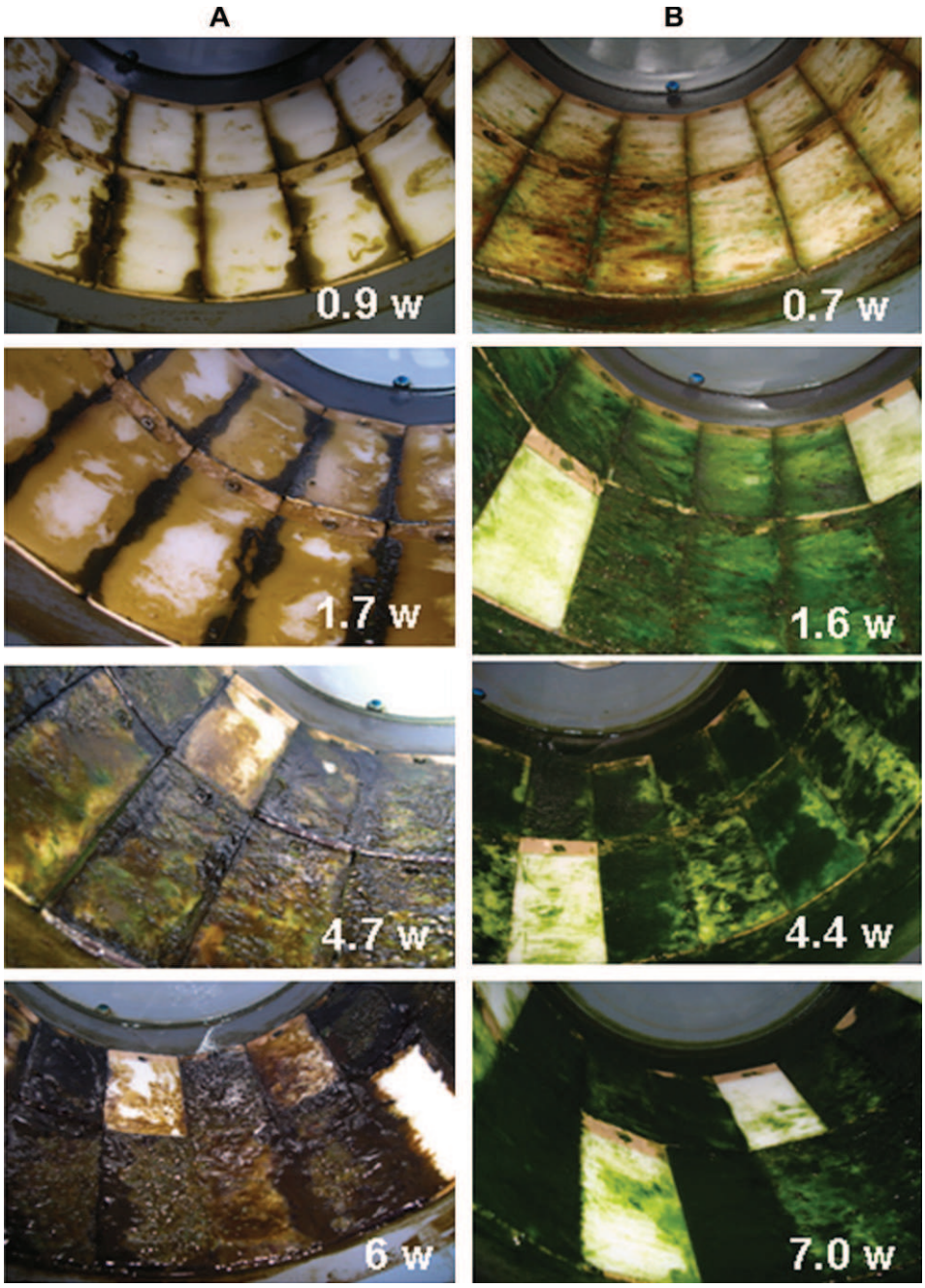

Fig. 5 – Photographic images of colonized plates on the internal surface of the external cylinder of the RAB during culture 1 (A) and culture 2 (B). Each plate has dimensions 50 × 100 mm^2. Numbers indicate biofilm age in weeks. White and partially colonized plates correspond to newly placed plates after sampling.

0.03 mg chlorophyll *a* cm^{-2} after 6 and 4.4 weeks of incubation for cultures 1 and 2 respectively (Figs. 6 and 7). This growth phase was followed by a plateau (Mann Whitney $p > 0.05$), then, for culture 2, by a slight loss of biomass (visible on the illustration of Fig. 5) (Mann Whitney, $p < 0.05$). Both variables (AFDM and chlorophyll *a*) were significantly correlated for the two cultures (C pearson = 0.95, $p < 0.01$ and C pearson = 0.93, $p < 0.01$, for cultures 1 and 2 respectively). The AFDM/DM ratio ranged from 39.5 to 62.1%, indicating biofilms poor in detritus and sedimentary particles (data not shown).

3.3.2. *Algal diversity*

Two seeding procedures were tested using inocula of different origins. The inoculum from artificial biofilm (experimental channel) used for culture 1 presented lower species richness (7 species) than the inoculum from natural biofilm (river) used for culture 2 (27 species). Moreover, the two inoculum types had different algal community compositions (Fig. 7). Inoculum from artificial biofilm was dominated by Cyanobacteria (95.4%) composed essentially of *Leptolyngbya* spp. (88.5%), and inoculum from natural biofilm was dominated by Diatoms

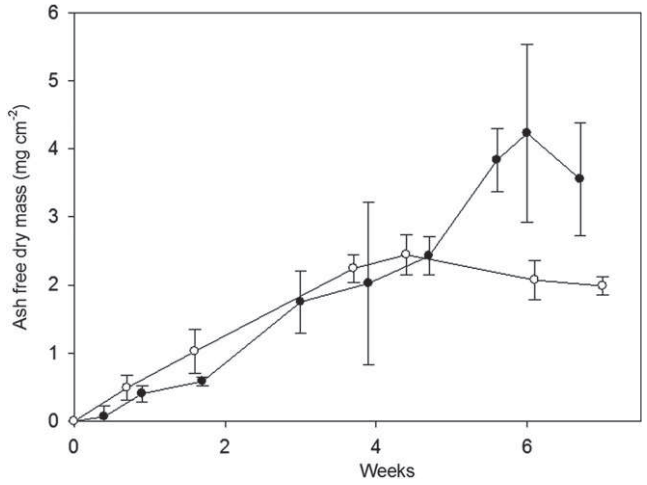

Fig. 6 – Temporal evolution of photosynthetic biofilm biomass expressed as mg cm^{-2} of ash-free dry mass (AFDM) during the growth period in bioreactor for culture 1 (black dots) and culture 2 (white dots).

(86.3%), composed essentially of *Navicula tripunctata* (O.F. Müller) Bory (23.2%), *Nitzschia* spp. (19.4%) and *Achnanthes* spp. (12.3%).

The species richness was relatively low and constant during culture 1 (from 5 to 7) although the species richness decreased over time during culture 2 (from 27 to 8). The 6.7-week mature biofilm from culture 1 was mainly composed of Diatoms (98.6%), especially *Nitzschia palea* (Kutz.) W. Smith (92.6%) and the mature biofilm from culture 2 was essentially composed of green algae (95.5%) especially *Scenedesmus* (74.9%) and *Ankistrodesmus/Monoraphidium* (9.9%). Six of the ten Chlorophyceae that composed the biofilm of culture 2 are known to present planktonic ecotypes.

3.3.3. *Bacterial community structure*

The dynamics of the bacterial community structure were determined by T-RFLP throughout the experiments. A total of 35 different T-RFs per culture for all sample times were identified with an average number per sample ranging from 12 to 25 and 12 to 23 T-RFs, for cultures 1 and 2 respectively. Principal component analysis (PCA) was performed on the T-RF binary data for each biofilm culture (Fig. 8). The two axes accounted for 21.2 and 18.6% of the total variance for culture 1, and 30.6 and 18.1% for culture 2. Good homogeneity was observed among replicates, particularly for culture 2, suggesting little spatial variability during the culture course in the bioreactor. This analysis was strengthened by the similar trends observed with PCAs built with the first and third axes. The first three axes accounted for 65.5 and 50.2% of the variation of T-RFLP patterns for cultures 1 and 2 (data not shown) respectively.

During both cultures, the bacterial community structure changed according to colonization time, based on sample clustering corresponding to a similarity of 55% (circle from Fig. 8) (culture 1 : global $R = 0.776$ and pairwise R ranged from 0.63 to 0.8, $p < 0.05$; culture 2 : global $R = 0.998$ and pairwise R ranged from 0.997 to 1, $p < 0.05$), followed by a stable phase after 3 weeks for culture 1 (global $R = 0.435$, $p < 0.05$) and 4.4 weeks for culture 2 (global $R = 0.51$, $p < 0.05$). Bacterial community composition rapidly diverged from the initial bacterial community (global $R = 0.895$ and 0.754, for cultures 1 and 2 respectively, $p < 0.05$). A PCA including T-RF of cultures 1 and 2 showed that the profiles were distributed along the first axis (28.9%) according to the origin of the inoculum (data not shown). PCA showed similar temporal variations of bacterial community structures during the biofilm development irrespective of the inoculum type.

4. Discussion

4.1. *Growth dynamics of phototrophic biofilms*

In environmental phototrophic biofilms, growth basically occurs through, firstly, an accretion phase related to colonization and growth processes (increase of AFDM resulting in a biomass peak) and, secondly, an ageing phase (Biggs, 1996).

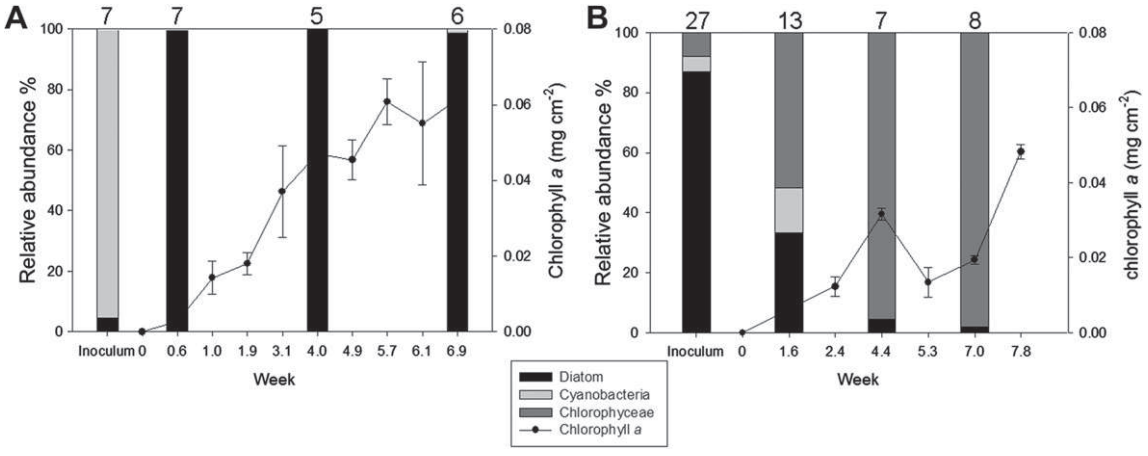

Fig. 7 – Temporal evolution of algal taxa number and their percentage abundance, and chlorophyll *a* as mg cm^{-2} of chlorophyll *a* during the biofilm growth period in RAB for cultures 1 (A) and 2 (B). The species richness is given for each sample at the bottom of each bar.

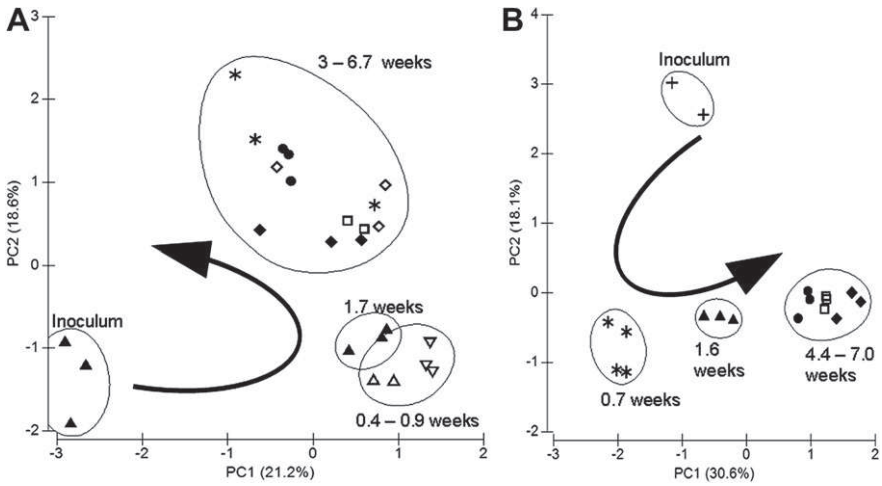

Fig. 8 – Changes in bacterial community structure over time assessed by Principal Component Analysis (PCA) based on the T-RFLP data for (A) culture 1 and (B) culture 2. Circles correspond to a similarity of 55%.

In the present experiments, linear growth phases were observed to reach AFDM peaks of 4.2 and 2.4 mg cm^{-2} after 6 and 4.4 weeks for cultures 1 and 2 respectively, followed by an ageing phase for culture 2. During the first step of each experiment, the colonization by suspended biomasses preferentially occurs on the substrate ridges. At the junction between two plates, the presence of gap was responsible for a recirculating flow near the solid surface. This stationary zone can act as a trap where biomass can accumulate, which could favour biofilm growth.

Typically, the first species to colonize the substrate are heterotrophic bacteria and algal with fast growth rate and small cells, followed by the settlement and colonization of slow growth and large cells species (Biggs et al., 1998; Sekar et al., 2002; Roeselers et al., 2007). Thus, Cyanobacteria are considered as late colonizers, with a slow growth rate (Sekar et al., 2002). This could explain their fast disappearance during both cultivations and their recurrence in the 6.7-week-old biofilm during culture 1. The use of a more diversified inoculum (natural) and longer seeding phase for culture 2 did not seem to enrich the algal community. As observed in most experiments performed at laboratory scale (Boulêtreau et al., 2010), biofilms at the end of the experiment exhibited poor algal specific richness, of 6 and 7 species for cultures 1 and 2 respectively. As a result, the minimal number of algal species to preserve an integral biofilm in this RAB seemed to be a final number of 6 or 7 species. The use of a single short seeding phase in the present work (48 h or twice 48 h) may have limited the adhesion of micro-organisms or only selected pioneer algal species and could thus be inherent to this poor diversity. The choice of constant experimental conditions during biofilm development did not favour environmental changes as observed in a natural environment (Biggs, 1996). It is known that, in an undisturbed environment (e.g. constant hydrodynamic conditions), autogenic processes appear and the more competitive species dominate (competitive exclusion), which can explain the poor algal diversity and lead to self detachment (Boulêtreau et al., 2006) as observed during culture 2 at 4.4 weeks of colonization. It has been suggested that initial high diversity is caused by the arrival of new micro-organisms, while ensuing competition decreases diversity in late successional stages (Sekar et al., 2002). In our RAB, the absence of arrival of new micro-organisms throughout experiment may have caused competition processes even during the first steps of colonization. In microcosm studies, the continuous seeding processes enable the natural conditions to be reproduced but can interact with the disturbance under study (Tlili et al., 2008).

The settings of the variables (temperature, light intensity, nutrient content, and flow rate), chosen to favour the growth of biofilms can be very selective for some species. For instance temperatures between 0 and 25 °C increased species richness and diversity and temperatures above 30 °C decreased species richness (DeNicola, 1996). Moreover, previous studies have shown that nutrient ratios (N, P and Si) greatly influence the composition of algal communities (Hillebrand and Sommer, 2000b) and that the enrichment of the medium favours the dominance of single species (Hillebrand and Sommer, 2000a).

End-of-experiment biofilms were strongly dominated either by *N. palea* (Kutz.) W. Smith. or *Scenedesmus* genus for culture 1 and culture 2, respectively. *N. palea* (Kutz.) W. Smith. and the *Scenedesmus* genus are eutrophic and polysaprobic species, which reveal nutrient-rich waters with strong conductivity (Tison et al., 2004; Peña-Castro et al., 2004). This is consistent with the physical-chemical characteristics of the culture medium used. *Scenedesmus* genus is a planktonic species and the seeding phase conducted in suspension could have induced its selection. The time taken to reach the AFDM peak was shorter for culture 2 than for culture 1 and was followed by a slight biomass removal leading to the ageing phase. Zippel and Neu (2005) concluded that green-algal-dominated biofilms presented a less stable and compact structure caused by a faster growth rate. The authors observed that fast development induced the formation of poorly diversified biofilms, probably explained by an economy and partition of resources (Zippel and Neu, 2005). One possible reason why algal diversity is small can be attributed to taxonomical analyses based on morphotypes. Many different

species can fall into the same category and can induce an under-estimation of specific richness.

Bacterial communities from both cultures changed markedly over the development of the biofilms. Despite differences in the inoculum communities, the succession was similar for both cultures associated with different trajectories. Since there was no addition of micro-organisms after the seeding phase, the temporal changes for algal and bacterial communities observed in the present study do not correspond to ecological succession processes occurring over natural biofilm maturation for either the algal (McCormick and Stevenson, 1991) or bacterial (Lyautey et al., 2005) compartments but are related to different algal species and T-RF dominance variations.

The primers used in this study have been designed to target specifically the Bacteria domain. Our *in silico* searches using the RDP database (Cole et al., 2009) indicated that both primers (8F and 1489R) can potentially target Cyanobacteria. Among the *in silico* targeted organisms, around 5% corresponded to cyanobacteria. Hence, the use of these primers in the current study could over-estimate non phototrophic bacteria richness.

4.2. *Rotating annular bioreactor*

4.2.1. *Improvements and advantages compared to other RAB*

Previous studies have suggested that the rotating annular bioreactor (RAB) can be an appropriate system to study the effects of various environmental factors on biofilm development (e.g. Neu and Lawrence, 1997; Chénier et al., 2003). Considering all critical points associated with RAB presented in the literature, the objective of this work was first to design an innovative bioreactor having a modular light source inside the system and second to have a good knowledge of hydrodynamic conditions as assessed using the numerical approach. Computer simulations allow us to confirm a turbulent vortex flow inside the annular gap with the presence of stacked vortices. We observed shear stress and velocity gradients at the scale of the vortices, and the distribution of shear stress described a periodic variation along the height of the bioreactor. As observed by Desmet et al. (1996), the presence of these vortices allows a faster real axial dispersion process than the plug-flow hydrodynamic type, which leads to well mixed liquid phase without of nutriment concentration gradients inside the annular gap, as verified by the tracer method. Variability between plates ($n = 3$) for the same sampling time was relatively low ($\leq$30%) for biomass analysis, and their percentage of homology was $\geq$60% for T-RFLP analysis, indicating low spatial variability of biofilm colonization and growth inside the RAB.

In ecological research, it is necessary to use controlled experiments with large replication to correct for the well known heterogeneity within biofilms (Wimpenny et al., 2000). Our prototype was therefore designed with numerous, large supports associated with a large liquid working volume (5.04 L). In fact, the 32 plates provided a total colonization surface of 0.16 m^2 in the present study as against the 12 plates providing 0.0132 m^2 of colonization surface in Lawrence et al. (2000), or the 20 plates with 0.00187 m^2 in Declerck et al. (2009). We used plates made of polyethylene, suggested to be applicable to the growth of bacterial (Yu et al., 2010) or phototrophic (Szlauer-Lukaszewska, 2007) biofilms. Their plastic nature and flexibility made them easy to curve so as to fit the external cylinder geometry, thus limiting the disturbance on the flow. The plate fixation design allowed quick and easy sampling without destruction of the sampled biofilms.

The geometry, current velocity and continuous culture mode of our prototype made it possible (i) to limit the development of phytoplankton and thus the competition processes between phototrophic biofilm and planktonic biomass, (ii) to limit potential erosion from recirculation of particle or sloughed biofilm fragments, and (iii) to avoid the settling of larger biofilm grazers in such an environment with fast rotation of the water column.

4.2.2. *Shortcomings and potential improvements*

The design of our RAB prototype leads to particular operating conditions for the phototrophic biofilm development. First, flow on the plates is produced by the rotation of the inner cylinder, and not directly by the circulation of the water through the system. The consequence is the RAB functioning as a partial closed flow through system without water contact with atmosphere, and with a water residence time of a few hours. The uncoupling between flow velocity on plates and medium flow rate gives unnatural operating conditions. For example, increases of pH (up to 10) or dissolved oxygen concentration (up to oversaturation of 200%) were obtained with daily variations and photosynthetic processes. These conditions may cause temporary inorganic carbon limitation, reactive oxygen damage, and selection of algal and bacterial species. To circumvent these shortcomings, a new version of the RAB must integrate pH control and oxygen stripping, for example with an external loop to prevent the modification of the flow pattern in the bioreactor. Second, the temperature is not controlled inside the bioreactor, and values up to 30 °C were obtained at the end of a diurnal period, or when the number of neon tubes was increased. Our RAB contains 3 cylinders, so the best way to control the temperature would be to thermoregulate the atmosphere inside the cylinder containing the neon tubes. Third, it can be suspected that a heterogenous distribution of light inside the RAB occurred, the total number of neon tubes being small and including two types of fluorescent lamps. This technical flaw can be circumvented by using opaque material placed inside the internal water-tight cylinder and in front of the lamps.

4.2.3. *Towards a promising tool*

In spite of some improvements needed on this prototype, our study presents the applicability and the performance of a new prototype of rotating annular bioreactor (Taylor–Couette flow type) which can be considered as a highly suitable tool for the cultivation, investigation and understanding of a variety of ecological concepts, including the specific richness–resistance relationship, or the coupling between hydrodynamic level/chemical compounds and structure/function of phototrophic biofilms.

As recorded in a previous study in microcosm (Boulêtreau et al., 2010), despite a poorly diversified algal community, the phototrophic biofilm exhibited high biomass production. This leads us to wonder about the effect of poor algal diversity

on the biomass production of phototrophic biofilm. A major challenge of the last decade has been to understand the relationship between diversity loss and ecosystem processes (Loreau et al., 2001). Numerous studies have shown that species-rich communities produce more biomass than species-poor communities (Zhang and Zhang, 2006). In future experiments, it could be interesting to assess the stability and resistance of these poorly diversified algal communities obtained in the prototype when a disturbance (e.g. toxic pollutants) is imposed on them. Various works have observed greater sensitivity to disturbance for poorly diversified communities (Zhang and Zhang, 2006).

Generally, it is difficult to individualize the main factors influencing epilithic biofilm development and several sources of stresses can have synergistic effects or the inverse. This prototype can bring new perspectives for characterizing the effect of a single factor (e.g. hydrodynamic). Through the ability to modulate the experimental conditions, and by the choice of a particular parameter adapted to algal ecology, the prototype can permit future investigations for the formation and cultivation of artificial biofilms as has recently been reported in the literature (Hayashi et al., 2010).

5. Conclusion

We propose an improved RAB featuring an embedded modular source of light and the possibility to accurately control the hydrodynamic conditions. These characteristics ensure better control of the operating conditions in comparison with other RABs. Additionally, the larger size of the bioreactor permits numerous samples of biomasses to be taken along the course of experiments to ensure replicates and long term cultures. Further improvements of our RAB version would be beneficial however, including technical solutions for temperature control, homogenous distribution of light inside the system, pH control and oxygen stripping, and operating conditions with a less selective culture medium and a continuous supply of biomass inoculum. Still, our RAB may be useful for the cultivation and experimental study of phototrophic biofilms. This approach is complementary to experimental and observational studies carried out at more complex and realistic scales such as 'open' channel and *in situ* investigations. Hence, RAB-based experiments can make a significant contribution to our understanding of the mechanisms which mediate the structure and functions of phototrophic biofilm communities.

Acknowledgements

This work was funded by the French National Programme EC2CO – Environmental Microbiology - and by the Midi-Pyrénées Council Programme of the Pyrenean working community. We are grateful to the ARIAS (Toulouse) company, especially J.-J.Bertrand, for manufacturing the rotating annular bioreactor. We thank J.-L. Druilhe for the electrical device for continuous physical-chemical measurement, S. Karama for assistance with the T-RFLP method, S. Mastrorillo for field assistance, and E. Mazeau for the computational study of hydrodynamics. We also thank D. Dalger and T. Louis for bioreactor handling assistance, and E. Lyautey for revising the correcting English of the manuscript.

REFERENCES

Battin, T.J., Kaplan, L.A., Newbold, J.D., Cheng, X., Hansen, C., 2003. Effects of current velocity on the nascent architecture of stream microbial biofilms. Applied and Environmental Microbiology 69 (9), 5443–5452.

Besemer, K., Singer, G., Limberger, R., Chlup, A.-K., Hochedlinger, G., Hödl, I., Baranyi, C., Battin, T.J., 2007. Biophysical controls on community succession in stream biofilms. Applied and Environmental Microbiology 73 (15), 4966–4974.

Biggs, B.J.F., 1996. Patterns in benthic algae of stream. In: Stevenson, R.J., Bothwell, M.L., Lowe, R.L. (Eds.), Algal Ecology. Freshwater Benthic Ecosystem. Academic Press, San Diego, pp. 31–56.

Biggs, B.J.F., Stevenson, R.J., Lowe, R.L., 1998. A habitat matrix conceptual model for stream periphyton. Archiv Für Hydrobiologie 143 (1), 21–56.

Boston, H.L., Hill, W.R., 1991. Photosynthesis-light relations of stream periphyton communities. Limnology and Oceanography 36 (4), 644–656.

Boulêtreau, S., Garabétian, F., Sauvage, S., Sánchez-Pérez, J.-M., 2006. Assessing the importance of a self-generated detachment process in river biofilm models. Freshwater Biology 51 (5), 901–912.

Boulêtreau, S., Sellali, M., Elosegi, A., Nicaise, Y., Bercovitz, Y., Moulin, F., Eiff, O., Sauvage, S., Sánchez-Pérez, J.-M., Garabétian, F., 2010. Temporal dynamics of river biofilm in constant flows: a case study in a riverside laboratory flume. International Review of Hydrobiology 95 (2), 156–170.

Bourassa, N., Cattaneo, A., 1998. Control of periphyton biomass in Laurentian streams (Québec). Journal of the North American Benthological Society 17 (4), 420–429.

Bruneel, O., Duran, R., Casiot, C., Elbaz-Poulichet, F., Personné, J.-C., 2006. Diversity of microorganisms in Fe–As-rich acid mine drainage waters of Carnoulès, France. Applied and Environmental Microbiology 72 (1), 551–556.

Characklis, W.G., 1990. Laboratory biofilm reactor. In: Characklis, W.G., Marshall, K.C. (Eds.), Biofilms. John Wiley and Sons, New York, pp. 55–89.

Chénier, M.R., Beaumier, D., Roy, R., Driscoll, B.T., Lawrence, J.R., Greer, C.W., 2003. Impact of seasonal variations and nutrient inputs on nitrogen cycling and degradation of hexadecane by replicated river biofilms. Applied and Environmental Microbiology 69 (9), 5170–5177.

Clarke, K.R., 1993. Non-parametric multivariate analyses of changes in community structure. Australian Journal of Ecology 18 (1), 117–143.

Cole, J.R., Wang, Q., Cardenas, E., Fish, J., Chai, B., Farris, R.J., Kulam-Syed-Mohideen, A.S., McGarrell, D.M., Marsh, T., Garrity, G.M., Tiedje, J.M., 2009. The ribosomal database project: improved alignments and new tools for rRNA analysis. Nucleic Acids Research 37 (suppl 1), D141–D145.

Coufort, C., Bouyer, D., Liné, A., 2005. Flocculation related to local hydrodynamics in a Taylor–Couette reactor and in a jar. Chemical Engineering Science 60 (8–9), 2179–2192.

Declerck, P., Behets, J., Margineanu, A., van Hoef, V., De Keersmaecker, B., Ollevier, F., 2009. Replication of *Legionella pneumophila* in biofilms of water distribution pipes. Microbiological Research 164 (6), 593–603.

DeNicola, D.M., 1996. Periphyton responses to temperature at different ecological levels. In: Stevenson, R.J., Bothwell, M.L., Lowe, R.L. (Eds.), Algal Ecology - Freshwater Benthic Ecosystems. Academic Press, San Diego, pp. 31–56.

Desmet, G., Verelst, H., Baron, G.V., 1996. Local and global dispersion effects in Couette–Taylor flow-II. Quantitative measurements and discussion of the reactor performance. Chemical Engineering Science 51 (8), 1299–1309.

Gjaltema, A., Arts, P.A.M., van Loosdrecht, M.C.M., Kuenen, J.G., Heijnen, J.J., 1994. Heterogeneity of biofilms in rotating annular reactors: occurrence, structure, and consequences. Biotechnology and Bioengineering 44 (2), 194–204.

Hammer, Y., Harper, D.A.T., Ryan, P.D., 2001. Past: paleontological statistics software package for education and data analysis. Palaeontologia Electronica 4 (1), 4–9.

Hayashi, S., Jang, J.E., Itoh, K., Suyama, K., Yamamoto, H., 2010. Construction of river model biofilm for assessing pesticide effects. Archives of Environmental Contamination and Toxicology 60 (1), 44–56.

Hillebrand, H., Sommer, U., 2000a. Diversity of benthic microalgae in response to colonization time and eutrophication. Aquatic Botany 67 (3), 221–236.

Hillebrand, H., Sommer, U., 2000b. Effect of continuous nutrient enrichment on microalgae colonizing hard substrates. Hydrobiologia 426 (1), 185–192.

Jackson, C.R., Churchill, P.F., Roden, E.E., 2001. Successional changes in bacterial assemblage structure during epilithic biofilm development. Ecology 82 (2), 555–566.

Lane, D.J., 1991. rRNA sequencing. In: Stachenbradt, E. (Ed.), Nucleic Acid Techniques in Bacterial Systematics. Wiley, Chichester, pp. 115–175.

Lawrence, J.R., Chénier, M.R., Roy, R., Beaumier, D., Fortin, N., Swerhone, G.D.W., Neu, T.R., Greer, C.W., 2004. Microscale and molecular assessment of impacts of nickel, nutrients, and oxygen level on structure and function of river biofilm communities. Applied and Environmental Microbiology 70 (7), 4326–4339.

Lawrence, J.R., Swerhone, G.D.W., Neu, T.R., 2000. A simple rotating annular reactor for replicated biofilm studies. Journal of Microbiological Methods 42 (3), 215–224.

Loreau, M., Naeem, S., Inchausti, P., Bengtsson, J., Grime, J.P., Hector, A., Hooper, D.U., Huston, M.A., Raffaelli, D., Schmid, B., Tilman, D., Wardle, D.A., 2001. Biodiversity and ecosystem functioning: current knowledge and future challenges. Science 294 (5543), 804–808.

Lyautey, E., Jackson, C.R., Cayrou, J., Rols, J.-L., Garabétian, F., 2005. Bacterial community succession in natural river biofilm assemblages. Microbial Ecology 50 (4), 589–601.

McCormick, P.V., Stevenson, R.J., 1991. Mechanisms of benthic algal succession in lotic environments. Ecology 72 (5), 1835–1848.

Murdock, J.N., Dodds, W.K., 2007. Linking benthic algal biomass to stream substratum topography. Journal of Phycology 43 (3), 449–460.

Neu, T.R., Lawrence, J.R., 1997. Development and structure of microbial biofilms in river water studied by confocal laser scanning microscopy. FEMS Microbiology Ecology 24 (1), 11–25.

Osborne, C.A., Rees, G.N., Bernstein, Y., Janssen, P.H., 2006. New threshold and confidence estimates for terminal restriction fragment length polymorphism analysis of complex bacterial communities. Applied and Environmental Microbiology 72 (2), 1270–1278.

Paule, A., Lyautey, E., Garabétian, F., Rols, J.-L., 2009. Autogenic *versus* environmental control during development of river biofilm. Annales de Limnologie-International Journal of Limnology 45 (1), 1–10.

Peña-Castro, J.M., Matínez-Jerónimo, F., Esparza-García, F., Cañizares-Villanueva, R.O., 2004. Phenotypic plasticity in *Scenedesmus incrassatulus* (Chlorophyceae) in response to heavy metals stress. Chemosphere 57 (11), 1629–1636.

Roeselers, G., van Loosdrecht, M.C.M., Muyzer, G., 2007. Heterotrophic pioneers facilitate phototrophic biofilm development. Microbial Ecology 54 (3), 578–585.

Sekar, R., Nair, K.V.K., Rao, V.N.R., Venugopalan, V.P., 2002. Nutrient dynamics and successional changes in a lentic freshwater biofilm. Freshwater Biology 47 (10), 1893–1907.

Singer, G., Besemer, K., Hödl, I., Chlup, A., Hochedlinger, G., Stadler, P., Battin, T.J., 2006. Microcosm design and evaluation to study stream microbial biofilms. Limnology and Oceanography: Methods 4, 436–447.

Smith, C.J., Danilowicz, B.S., Clear, A.K., Costello, F.J., Wilson, B., Meijer, W.G., 2005. T-Align, a web-based tool for comparison of multiple terminal restriction fragment length polymorphism profiles. FEMS Microbiology Ecology 54 (3), 375–380.

Sugiharto, S., Su'ud, Z., Kurniadi, R., Wibisono, W., Abidin, Z., 2009. Radiotracer method for residence time distribution study in multiphase flow system. Applied Radiation and Isotopes 67 (7–8), 1445–1448.

Szlauer-Lukaszewska, A., 2007. Succession of periphyton developing on artificial substrate immersed in polysaprobic wastewater reservoir. Polish Journal of Environmental Studies 16 (5), 753–762.

Tison, J., Giraudel, J.L., Coste, M., Park, Y.-S., Delmas, F., 2004. Use of unsupervised neural networks for ecoregional zoning of hydrosystems through diatom communities: case study of Adour-Garonne watershed (France). Archiv Für Hydrobiologie 159 (3), 409–422.

Tlili, A., Dorigo, U., Montuelle, B., Margoum, C., Carluer, N., Gouy, V., Bouchez, A., Bérard, A., 2008. Responses of chronically contaminated biofilms to short pulses of diuron: an experimental study simulating flooding events in a small river. Aquatic Toxicology 87 (4), 252–263.

Utermöhl, H., 1958. Zur vervollkommnung der quantitativen phytoplankton methodik. Mitteilungen Internationale Vereinigung für Theoretische und Angewandte Limnologie 9, 1–38.

Weisburg, W.G., Barns, S.M., Pelletier, D.A., Lane, D.J., 1991. 16S ribosomal DNA amplification for phylogenetic study. The Journal of Bacteriology 173 (2), 697–703.

Wimpenny, J., Manz, W., Szewzyk, U., 2000. Heterogeneity in biofilms. FEMS Microbiology Reviews 24 (5), 661–671.

Yu, J., Kim, D., Lee, T., 2010. Microbial diversity in biofilms on water distribution pipes of different materials. Water Science and Technology 61 (1), 163–171.

Zhang, Q.-G., Zhang, D.-Y., 2006. Species richness destabilizes ecosystem functioning in experimental aquatic microcosms. Oikos 112 (1), 218–226.

Zippel, B., Neu, T.R., 2005. Growth and structure of phototrophic biofilms under controlled light conditions. Water Science and Technology 52 (7), 203–209.